Available online at http://scik.org
Commun. Math. Biol. Neurosci. 2024, 2024:81
https://doi.org/10.28919/cmbn/8690
ISSN: 2052-2541

THE DYNAMICS OF INFLUENZA AND COVID-19 COINFECTION WITH VACCINATION: STABILITY AND SENSITIVITY

JONNER NAINGGOLAN[1,*], MOCH. FANDI ANSORI[2], FELICIA AGATHA WENEHEN[3], ANTONIA G. N. M. PANJAITAN[3]

[1]Department of Mathematics, Faculty of Mathematics and Natural Sciences, Universitas Cenderawasih, Jayapura 99224, Indonesia

[2]Department of Mathematics, Faculty of Science and Mathematics, Universitas Diponegoro, Semarang 50275, Indonesia

[3]Undergraduate Study Program of Mathematics, Faculty of Mathematics and Natural Sciences, Universitas Cenderawasih, Jayapura 99224, Indonesia

Abstract. A mathematical model of influenza and COVID-19 coinfection is considered. We add a vaccinated subpopulation, where the vaccine is applied to both diseases. We analyse the solution's positivity and the local stability of the equilibrium. The basic reproduction ratio is calculated using the next-generation matrix resulting in a maximum value between the basic reproduction ratio of influenza and COVID-19. It is found that the non-endemic equilibrium point is locally asymptotically stable if the basic reproduction ratio is less than one. Some numerical simulations are performed, and a sensitivity analysis is given. The result suggests that the regulator needs to pay attention to curbing the interaction of infected subpopulations and boosting the influenza recovery rate to control the disease spread.

Keywords: COVID-19; coinfection; influenza; sensitivity.

2020 AMS Subject Classification: 37N25, 93B35.

*Corresponding author

E-mail address: jonner2766@gmail.com

Received June 10, 2024

1. INTRODUCTION

Influenza and COVID-19 are contagious respiratory illnesses that have been the focus of extensive scientific investigations. Mathematical modelling is crucial for comprehending the dynamics of disease transmission, as well as for assessing and forecasting the course of the epidemic and measures for controlling it. Mathematical models of influenza or COVID-19 transmission are crucial for research because of the progressive nature of the disease and the continuous advancements in science and technology.

By conducting modelling studies and analysing the dynamics of influenza dissemination, researchers can gain insights into its transmission and develop effective prevention techniques [1]. The dynamics of influenza propagation are intricate and can be counterintuitive, making it challenging to explain using basic influenza models. However, the model can be evaluated to ensure its accuracy [2]. An influenza infection overview presents a comprehensive account of the initial symptoms, recurrent infections, and their impact on the human body [3]. To comprehend the dynamics of influenza and bird flu, it is imperative to investigate the transmission variables and subpopulations associated with their distribution model. This is because both diseases exhibit nearly identical distribution patterns [4]. The human respiratory system serves as the pathway for viral infections to enter the human body. Therefore, it is crucial to maintain a sanitary environment in the vicinity of the nose and mouth [5]. Individuals who are afflicted with influenza and do not receive proper treatment or fail to complete a course of antibiotics, may develop resistance to influenza medications [6].

Vaccination is a more effective method than therapy for preventing the spread of influenza [7]. In order to address influenza that is resistant to anti-influenza medications, mathematical analysis has determined that effective pharmaceuticals must be utilised for therapy [8]. The management of influenza can be revolutionised by using impulse-based control techniques, which offer optimal therapeutic innovations [9].

Over the past few years, the emergence of the novel coronavirus SARS-CoV-2, often known as COVID-19, has had an unprecedented influence on global issues. Several meticulous scientific investigations and analyses have been conducted to comprehend its dynamics, in order to contribute to public health policy. To comprehensively understand and effectively manage

the transmission of the virus, it is imperative for mathematical scientists to engage in collaborative efforts with the health sector to conduct preliminary analysis. This early study serves as a crucial step in addressing the challenges posed by COVID-19. Research has been conducted to examine the dynamics of COVID-19 and the effectiveness of preventative measures, such as social restrictions, lockdowns, and treatment, in reducing the death rate caused by the disease. The aim of these studies is to provide recommendations on how to effectively prevent COVID-19 [10].

Mathematical studies that aim to forecast the transmission of COVID-19 can provide outcomes that carry substantial consequences for public health strategies and the distribution of resources for response efforts [11]. In Indonesia, researchers have conducted studies on distribution prediction models using the Susceptible-Infected-Recovered (SIR) model [12]. They have also performed sensitivity analysis to examine the impact of comorbid disease factors on disease spread [13]. Additionally, they have explored the selection of recruitment in susceptible subpopulations using logistic growth [14]. The field of mathematical epidemiology in the context of COVID-19 provides an overview of the essential factors and compartments involved in the transmission of the virus. This knowledge serves as a foundation for developing effective strategies to manage the ongoing pandemic [15].

Furthermore, mathematical modelling plays a crucial role in comprehending the interactions between SARS-CoV-2 and other viruses. Specifically, it aims to elucidate the dynamics of the intricate viral interference, which is a critical factor in understanding the co-infection of COVID-19 and other respiratory diseases. Mathematical modelling has been used to analyse the interactions between different infectious agents [16]. It is necessary to study the co-infection of COVID-19 and influenza in order to determine the most suitable healthcare system for allocating resources during simultaneous epidemics [17].

Research is examined to study the impact of vaccine interventions on the spread of COVID-19. It also highlighted the significant significance of vaccination campaigns in raising awareness about the need of immunisation in preventing the disease from spreading further [18]. A study was conducted to investigate the impact of health protocol campaigns on the prevention of COVID-19 and influenza co-infection. Nonlinear models were used to analyse the spread of

both diseases and determine the optimal control measures. The study examined the effects of preventive strategies on each disease separately as well as when they occur together [19]. This research expands upon the model examined by Bhowmick (2023) [17] by including subpopulations related to vaccination. The inclusion of the vaccine component is crucial as immunisation serves as a highly effective measure in mitigating the transmission of COVID-19 or influenza. This is consistent with research undertaken in other studies [7, 14, 18, 19].

2. THE MODEL

We consider a coinfection model of COVID-19 and Influenza by extending the model in Bhowmick (2023) [17] by adding a vaccinated subpopulation.

Suppose a population, denoted by N which is assumed to be a constant, is divided into six subpopulations. The susceptible subpopulation denoted by S refers to persons who are currently in good health but are at risk of contracting either COVID-19 or influenza. The vaccinated subpopulation denoted by V refers to persons who are susceptible to influenza and COVID-19 despite being vaccinated with the influenza vaccine and COVID-19 vaccine. The influenza-infected subpopulation denoted by I_F refers to persons who are only infected by the influenza virus. The COVID-19-infected subpopulation denoted by I_C refers to persons who are only infected by the COVID-19 virus. The influenza and COVID-19 co-infected subpopulation denoted by I_{FC} refers to persons who are infected by both influenza and COVID-19 viruses. The recovered subpopulation denoted by R are persons who have acquired immunity either by vaccination, spontaneous infection, or recovery from treatment.

The transmission diagram of the population is given in Fig. 1. The explanation of the figure is as follows:

1. All subpopulations have a natural death rate μ.
2. S has a recruitment rate Λ, a influenza infection transition rate β_1/N, a COVID-19 infection transition rate β_2/N, a influenza vaccination rate ψ, and a COVID-19 vaccination rate ω.
3. V has influenza infection transition rate β_3/N and a COVID-19 infection transition rate β_4/N. V can be fully recovered from influenza at the rate r_1 and from COVID-19 at the rate r_2.

4. I_F has a coinfection rate with COVID-19 at γ and can be fully recovered by another factor except for vaccination at the rate σ.
5. I_C has a coinfection rate with influenza at δ, a death rate caused by COVID-19 at d_1, and can be fully recovered by another factor except for vaccination at the rate τ.
6. I_{FC} can be fully recovered by another factor except for vaccination at the rate φ and has a death rate caused by the coinfection at d_2.

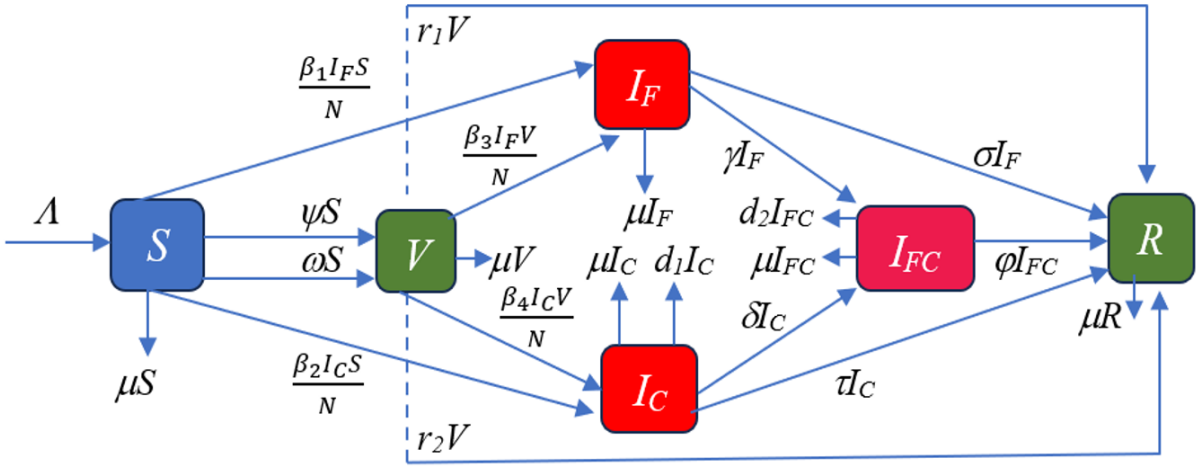

FIGURE 1. The transmission of the coinfection of influenza and COVID-19.

Based on the above explanation of the coinfection dynamics of influenza and COVID-19, we have the following system of differential equations:

$$
(1)\qquad
\begin{cases}
\frac{dS}{dt} = \Lambda - \left(\frac{\beta_1}{N} I_F + \frac{\beta_2}{N} I_C + \psi + \omega + \mu\right) S \\
\frac{dV}{dt} = (\psi + \omega) S - \left(\frac{\beta_3}{N} I_F + \frac{\beta_4}{N} I_C + r_1 + r_2 + \mu\right) V \\
\frac{dI_F}{dt} = \left(\frac{\beta_1}{N} S + \frac{\beta_3}{N} V\right) I_F - (\gamma + \sigma + \mu) I_F \\
\frac{dI_C}{dt} = \left(\frac{\beta_2}{N} S + \frac{\beta_4}{N} V\right) I_C - (d_1 + \delta + \tau + \mu) I_C \\
\frac{dI_{FC}}{dt} = \gamma I_F + \delta I_C - (\varphi + d_2 + \mu) I_{FC} \\
\frac{dR}{dt} = (r_1 + r_2) V + \sigma I_F + \tau I_C + \varphi I_{FC} - \mu R
\end{cases}
$$

The total population is $N = S + V + I_F + I_C + I_{FC} + R$. In Table 1, we provide the parameters' description, value (for simulation purposes), and reference.

TABLE 1. The description and value of the parameters.

Parameter	Description	Value	Ref.
Λ	Recruitment rate	1.2×10^4	[19]
β_1	Influenza infection transition rate from susceptible subpopulation	0.203	[19]
β_2	COVID-19 infection transition rate from susceptible subpopulation	0.5249	[19]
ψ	Influenza vaccination rate	0.00027	[19]
ω	COVID-19 vaccination rate	0.0203	[19]
β_3	Influenza infection transition rate from vaccinated subpopulation	0.035	[17]
β_4	COVID-19 infection transition rate from vaccinated subpopulation	0.021	[17]
r_1	Vaccinated subpopulation recovery rate from influenza	0.7	Assumed
r_2	Vaccinated subpopulation recovery rate from COVID-19	0.011	[19]
γ	Influenza-infected coinfection rate with COVID-19	0.088	[19]
σ	Recovery rate of the influenza-infected subpopulation by another factor except for vaccination	0.77	Assumed
δ	COVID-19-infected coinfection rate with influenza	0.4	Assumed
d_1	Death rate caused by COVID-19	0.008	[19]
τ	Recovery rate of the COVID-19-infected subpopulation by another factor except for vaccination	0.1398	[19]
φ	Recovery rate of the coinfected subpopulation by another factor except for vaccination	0.125	Assumed
d_2	Death rate caused by the coinfection	0.021	Assumed
μ	Natural death rate	0.00004	Assumed

We assume that all parameters are non-negative and the initial value of all subpopulations are non-negative except $S(0) > 0$.

2.1. Stability Analysis. We have the following theorem about the non-negativity of the system (1) solutions.

Theorem 2.1. *Given $S(0) > 0$ and $V(0), I_F(0), I_C(0), I_{FC}(0), R(0) \geq 0$, the solutions of system (1) are non-negative, that is $S(t), V(t), I_F(t), I_C(t), I_{FC}(t), R(t) \geq 0$ for all $t > 0$.*

Proof. Let $\tilde{t} = \sup\{t > 0 | S(0), V(0), I_F(0), I_C(0), I_{FC}(0), R(0) > 0\} \in [0, t]$. From the first differential equation in (1), we have

$$\frac{dS}{dt} \geq \Lambda - \left(\frac{\beta_1}{N} I_F + \frac{\beta_2}{N} I_C + \mu\right) S.$$

By using a factor integration technique, the solution of the above inequality is

$$S(\tilde{t}) \geq \left[S(0) + \int_0^{\tilde{t}} \Lambda \exp\left(\mu\tilde{t} + \int_0^{\tilde{t}} (\xi_1(u) + \xi_2(u)) du\right) d\tilde{t}\right] \exp\left[-\left(\mu\tilde{t} + \int_0^{\tilde{t}} (\xi_1(s) + \xi_2(s)) ds\right)\right].$$

This means that $S(\tilde{t}) > 0$, for all $t > 0$. In the same way, we can obtain $V(\tilde{t}), I_F(\tilde{t}), I_C(\tilde{t}), I_{FC}(\tilde{t}), R(\tilde{t}) \geq 0$, for all $t > 0$. □

The non-endemic equilibrium can be obtained if the infected subpopulations are zero. We get

$$E_0 = \left(\frac{\Lambda}{\psi + \omega + \mu}, \frac{\Lambda(\psi + \omega)}{(\psi + \omega + \mu)(r_1 + r_2 + \mu)}, 0, 0, 0, \frac{\Lambda(\psi + \omega)(r_1 + r_2)}{\mu(\psi + \omega + \mu)(r_1 + r_2 + \mu)}\right).$$

The magnitude of the expansion or contraction of a disease's transmission within a population can be ascertained by examining the value of the basic reproduction ratio. The basic reproduction ratio, denoted by $\mathscr{R}_0$, represents the average number of infected people that arise from a single infected individual entering each susceptible subpopulation. The basic reproduction ratio of system (1) is determined using the next-generation matrix approach [20]. Firstly, let us examine the Jacobian matrix of a system consisting of infected individuals who are in contact with susceptibles at the non-endemic equilibrium point.

$$F = \begin{bmatrix} \frac{\beta_1 \Lambda}{N(\gamma+\sigma+\mu)} + \frac{\beta_3 \Lambda(\psi+\omega)}{N(\psi+\omega+\mu)(r_1+r_2+\mu)} & 0 & 0 & 0 \\ 0 & \frac{\beta_2 \Lambda}{N(\gamma+\sigma+\mu)} + \frac{\beta_4 \Lambda(\psi+\omega)}{N(\psi+\omega+\mu)(r_1+r_2+\mu)} & 0 & 0 \\ 0 & 0 & 0 & 0 \\ 0 & 0 & 0 & 0 \end{bmatrix}$$

The Jacobian matrix of which individuals are exiting the system without coming into touch with infected individuals is given below

$$V = \begin{bmatrix} \gamma+\sigma+\mu & 0 & 0 & 0 \\ 0 & d_1+\delta+\tau+\mu & 0 & 0 \\ -\gamma & -\delta & \varphi+d_2+\mu & \\ -\sigma & -\tau & -\varphi & \mu \end{bmatrix}$$

The basic reproduction number of system (1) is obtained by calculating the spectral radius of the matrix FV^{-1}. Since there are two infectious diseases, influenza and COVID-19, then we have

$$\mathscr{R}_0 = \max\{\mathscr{R}_{0F}, \mathscr{R}_{0C}\},$$

where

$$\mathscr{R}_{0F} = \left(\frac{\mu}{\gamma+\sigma+\mu}\right)\left(\frac{\beta_1}{\gamma+\sigma+\mu} + \frac{\beta_3(\psi+\omega)}{(\psi+\omega+\mu)(r_1+r_2+\mu)}\right)$$

is the basic reproduction ratio of influenza, and

$$\mathscr{R}_{0C} = \left(\frac{\mu}{d_1+\delta+\tau+\mu}\right)\left(\frac{\beta_2}{\gamma+\sigma+\mu} + \frac{\beta_4(\psi+\omega)}{(\psi+\omega+\mu)(r_1+r_2+\mu)}\right)$$

is the basic reproduction ratio of COVID-19.

The connection between the stability of the non-endemic equilibrium point and the basic reproduction ratio is given in the following theorem.

Theorem 2.2. *The non-endemic equilibrium point E_0 is locally asymptotically stable if $\mathscr{R}_0 < 1$, and unstable otherwise.*

Proof. Consider the Jacobian matrix of system (1) evaluated at E_0,

$$J(E_0) = \begin{bmatrix} -a & 0 & -\frac{\beta_1\mu}{a} & -\frac{\beta_2\mu}{a} & 0 & 0 \\ \psi+\omega & -b & -\frac{\beta_3\mu(\psi+\omega)}{ab} & -\frac{\beta_4\mu(\psi+\omega)}{ab} & 0 & 0 \\ 0 & 0 & \frac{\mu\beta_1}{a} + \frac{\beta_3\mu(\psi+\omega)}{ab} - c & 0 & 0 & 0 \\ 0 & 0 & 0 & \frac{\mu\beta_2}{a} + \frac{\beta_4\mu(\psi+\omega)}{ab} - d & 0 & 0 \\ 0 & 0 & \gamma & \delta & -e & 0 \\ 0 & r_1+r_2 & \sigma & \tau & \varphi & -\mu \end{bmatrix}$$

where $a = \psi + \omega + \mu$, $b = r_1 + r_2 + \mu$, $c = \gamma + \sigma + \mu$, $d = d_1 + \delta + \tau + \mu$, and $e = \varphi + d_2 + \mu$. Note that $a, b, c, d, e > 0$. The eigenvalues of the Jacobian matrix $J(E_0)$ are obtained as follows

$$\lambda_1 = -e, \lambda_2 = -\mu, \lambda_3 = -b, \lambda_4 = \frac{\mu\beta_2}{a} + \frac{\beta_4\mu(\psi+\omega)}{ab} - d$$
$$\lambda_5 = \frac{\mu\beta_1}{a} + \frac{\beta_3\mu(\psi+\omega)}{ab} - c, \lambda_6 = -a.$$

If $d > \frac{\mu\beta_2}{a} + \frac{\beta_4\mu(\psi+\omega)}{ab}$ and $c > \frac{\mu\beta_1}{a} + \frac{\beta_3\mu(\psi+\omega)}{ab}$, then all the eigenvalues are negative which means that E_0 is stable. One can observe that these two conditions are equivalent with $\mathscr{R}_0 < 1$. Thus, E_0 is stable if $\mathscr{R}_0 < 1$. □

The study of the endemic equilibrium is not presented in this paper, because it has long expression and requires comprehensive analysis. We leave it for further study.

3. Simulations and Sensitivity Analysis

In this section, we perform some simulations of the system (1) solution and also provide a sensitivity analysis to observe which parameter is the most sensitive or influential to the disease spread.

We use the parameters' value from Table 1 and the following initial conditions that are only chosen for simulation purposes: $S(0) = 2 \times 10^8$, $V(0) = 1.5 \times 10^8$, $I_F(0) = 3.1 \times 10^5$, $I_C(0) = 3.2 \times 10^5$, $I_{FC}(0) = 1 \times 10^3$, $R(0) = 5.4 \times 10^6$. First, we simulate the system's time series solution in Fig. 2a for the non-infected subpopulations S, V, and R, and in Fig. 2b for the infected subpopulations I_F, I_C, and I_{FC}. The susceptible and vaccinated subpopulations tend to decrease, on the other hand, the recovered subpopulation tends to grow until reaching its steady state. The influenza-infected and COVID-19-infected subpopulations tend to decrease from the start, meanwhile, the coinfected subpopulation tends to grow initially but decreases after that. These three infected subpopulations converge to zero at the end. This is confirmed by the basic reproduction ratio which is less than one. For another representation of the system (1) solution, in Fig. 3, we present a phase diagram of the vaccinated subpopulation V with the infected subpopulation I_F, I_C, and I_{FC}. The simulation is performed with various initial conditions.

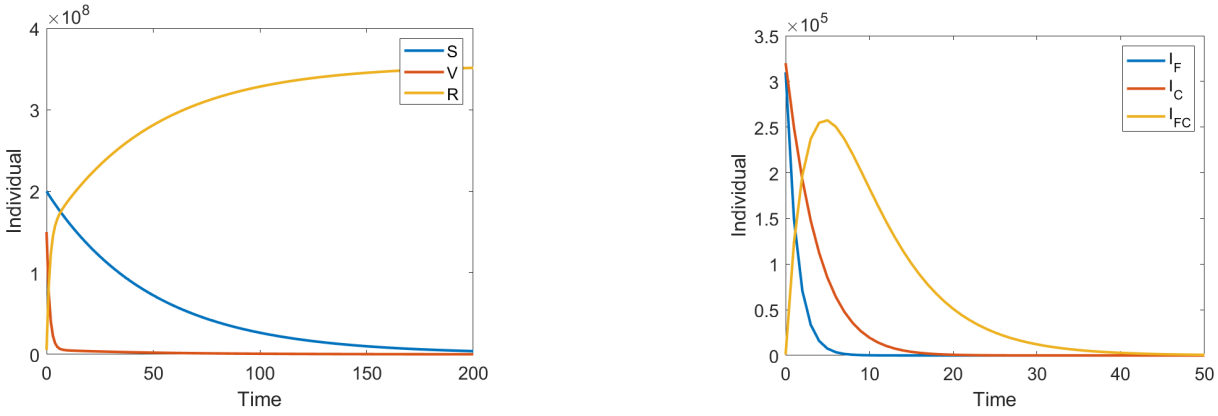

(A) (B)

FIGURE 2. The solution of system (1) (a) for non-infected subpopulations S, V, and R, and (b) for infected subpopulations I_F, I_C, and I_{FC}.

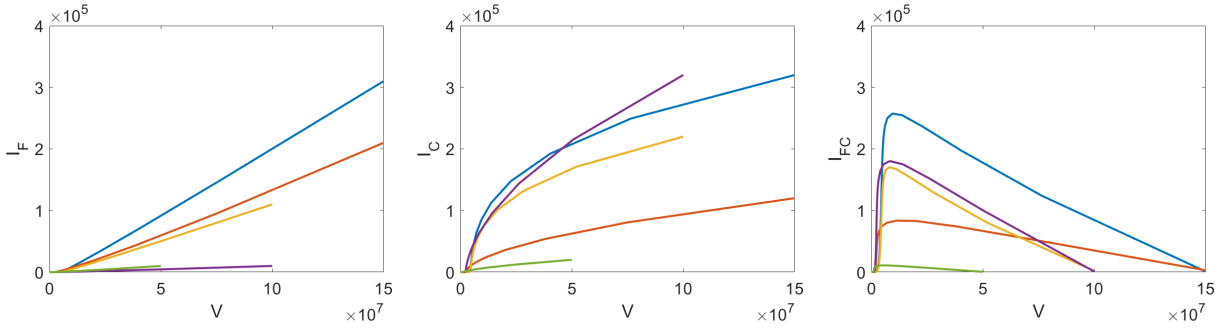

(A) (B) (C)

FIGURE 3. The phase diagram of the vaccinated subpopulation V versus the infected subpopulations (a) I_F, (b) I_C, and (c) I_{FC}. The simulation uses various initial values.

3.1. Sensitivity Analysis. One of the important analyses in mathematical epidemiology is sensitivity analysis which is to observe the most influential parameters that contribute to the disease spread. The sensitivity analysis that we considered here is an elasticity index which is defined as follows

$$E = \frac{\partial \mathscr{R}_0}{\partial P} \times \frac{P}{\mathscr{R}_0},$$

where P is the parameter that appear in $\mathscr{R}_0$. In this paper, we have

$$P \in \{\beta_1, \beta_2, \psi, \omega, \beta_3, \beta_4, r_1, r_2, \gamma, \sigma, \delta, d_1, \tau, \mu\}.$$

The calculation result of the elasticity index is given in Table 2. Bu using the parameters' value from Table 1, we have the result comparison of the elasticity index of all parameters given in Fig. 4. From the figure, we can observe that parameter μ is the most sensitive, followed by parameters β_2, σ, and β_1.

TABLE 2. Elasticity index calculation.

Parameter	Elasticity index
β_1	$\frac{\mu}{(\gamma+\mu+\sigma)^2}$
β_2	$\frac{\mu}{(\gamma+\mu+\sigma)(d_1+\delta+\mu+\tau)}$
ψ	$\max\left\{\frac{\mu\left(\frac{\beta_3}{(\mu+\omega+\psi)(\mu+r_1+r_2)}-\frac{\beta_3(\omega+\psi)}{(\mu+\omega+\psi)^2(\mu+r_1+r_2)}\right)}{\gamma+\mu+\sigma}, \frac{\mu\left(\frac{\beta_4}{(\mu+\omega+\psi)(\mu+r_1+r_2)}-\frac{\beta_4(\omega+\psi)}{(\mu+\omega+\psi)^2(\mu+r1+r_2)}\right)}{d_1+\delta+\mu+\tau}\right\}$
ω	$\max\left\{\frac{\mu\left(\frac{\beta_3}{(\mu+\omega+\psi)(\mu+r_1+r_2)}-\frac{\beta_3(\omega+\psi)}{(\mu+\omega+\psi)^2(\mu+r_1+r_2)}\right)}{\gamma+\mu+\sigma}, \frac{\mu\left(\frac{\beta_4}{(\mu+\omega+\psi)(\mu+r_1+r_2)}-\frac{\beta_4(\omega+\psi)}{(\mu+\omega+\psi)^2(\mu+r_1+r_2)}\right)}{d_1+\delta+\mu+\tau}\right\}$
β_3	$\frac{\mu(\omega+\psi)}{(\gamma+\mu+\sigma)(\mu+\omega+\psi)(\mu+r_1+r_2)}$
β_4	$\frac{\mu(\omega+\psi)}{(\mu+\omega+\psi)(\mu+r_1+r_2)(d_1+\delta+\mu+\tau)}$
r_1	$\max\left\{\frac{\beta_3\mu(\omega+\psi)}{(\gamma+\mu+\sigma)(\mu+\omega+\psi)(\mu+r_1+r_2)^2}, \frac{\beta_4\mu(\omega+\psi)}{(\mu+\omega+\psi)(\mu+r_1+r_2)^2(d_1+\delta+\mu+\tau)}\right\}$
r_2	$\max\left\{\frac{\beta_3\mu(\omega+\psi)}{(\gamma+\mu+\sigma)(\mu+\omega+\psi)(\mu+r_1+r_2)^2}, \frac{\beta_4\mu(\omega+\psi)}{(\mu+\omega+\psi)(\mu+r_1+r_2)^2(d_1+\delta+\mu+\tau)}\right\}$
γ	$\max\left\{\frac{\mu\left(\frac{\beta_1}{\gamma+\mu+\sigma}+\frac{\beta_3(\omega+\psi)}{(\mu+\omega+\psi)(\mu+r_1+r_2)}\right)}{(\gamma+\mu+\sigma)^2}-\frac{\beta_1\mu}{(\gamma+\mu+\sigma)^3}, -\frac{\beta_2\mu}{(\gamma+\mu+\sigma)^2(d_1+\delta+\mu+\tau)}\right\}$
σ	$\max\left\{-\frac{\mu\left(\frac{\beta_1}{\gamma+\mu+\sigma}+\frac{\beta_3(\omega+\psi)}{(\mu+\omega+\psi)(\mu+r_1+r_2)}\right)}{(\gamma+\mu+\sigma)^2}-\frac{\beta_1\mu}{(\gamma+\mu+\sigma)^3}, -\frac{\beta_2\mu}{(\gamma+\mu+\sigma)^2(d_1+\delta+\mu+\tau)}\right\}$
δ	$\frac{\mu\left(\frac{\beta_2}{\gamma+\mu+\sigma}+\frac{\beta_4(\omega+\psi)}{(\mu+\omega+\psi)(\mu+r_1+r_2)}\right)}{(d_1+\delta+\mu+\tau)^2}$
d_1	$-\frac{\mu\left(\frac{\beta_2}{\gamma+\mu+\sigma}+\frac{\beta_4(\omega+\psi)}{(\mu+\omega+\psi)(\mu+r_1+r_2)}\right)}{(d_1+\delta+\mu+\tau)^2}$
τ	$-\frac{\mu\left(\frac{\beta_2}{\gamma+\mu+\sigma}+\frac{\beta_4(\omega+\psi)}{(\mu+\omega+\psi)(\mu+r_1+r_2)}\right)}{(d_1+\delta+\mu+\tau)^2}$
μ	$\max\left\{\frac{\beta_1}{\gamma+\mu+\sigma}+\frac{\beta_3(\omega+\psi)}{(\mu+\omega+\psi)(\mu+r_1+r_2)}-\frac{\mu\left(\frac{\beta_1}{\gamma+\mu+\sigma}+\frac{\beta_3(\omega+\psi)}{(\mu+\omega+\psi)(\mu+r_1+r_2)}\right)}{(\gamma+\mu+\sigma)^2}\right.$ $-\frac{\mu\left(\frac{\beta_1}{(\gamma+\mu+\sigma)^2}+\frac{\beta_3(\omega+\psi)}{(\mu+\omega+\psi)(\mu+r_1+r_2)^2}+\frac{\beta_3(\omega+\psi)}{(\mu+\omega+\psi)^2(\mu+r_1+r_2)}\right)}{\gamma+\mu+\sigma}$, $\frac{\beta_2}{\gamma+\mu+\sigma}+\frac{\beta_4(\omega+\psi)}{(\mu+\omega+\psi)(\mu+r_1+r_2)}-\frac{\mu\left(\frac{\beta_2}{\gamma+\mu+\sigma}+\frac{\beta_4(\omega+\psi)}{(\mu+\omega+\psi)(\mu+r_1+r_2)}\right)}{(d_1+\delta+\mu+\tau)^2}$ $\left.-\frac{\mu\left(\frac{\beta_2}{(\gamma+\mu+\sigma)^2}+\frac{\beta_4(\omega+\psi)}{(\mu+\omega+\psi)(\mu+r_1+r_2)^2}+\frac{\beta_4(\omega+\psi)}{(\mu+\omega+\psi)^2(\mu+r_1+r_2)}\right)}{d_1+\delta+\mu+\tau}\right\}$

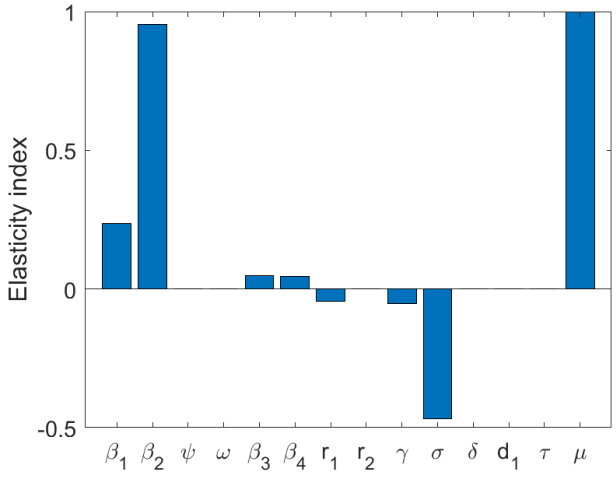

FIGURE 4. The elasticity index of the basic reproduction ration $\mathscr{R}_0$ for all parameters that appear in $\mathscr{R}_0$.

4. CONCLUSION

Based on the given parameters' value, to overcome the disease spread, we should pay attention to the natural death rate, COVID-19 infection transition rate, recovery rate of the influenza-infected, and influenza infection transition rate. Indeed, as the health regulator, they can not control the natural death rate. Still, they can make regulations to curb the COVID-19 and influenza infection transition rates and also boost the recovery rate of influenza-infected people.

ACKNOWLEDGMENTS

The author expresses gratitude to Kemenristek Dikti for providing the Penelitian Fundamental Reguler (PFR) BIMA Grants for Fiscal 2024, which were sponsored by LPPM Universitas Cenderawasih for this work.

CONFLICT OF INTERESTS

The authors declare that there is no conflict of interests.

REFERENCES

[1] D. Guo, K.C. Li, T.R. Peters, et al. Multi-scale modeling for the transmission of influenza and the evaluation of interventions toward it, Sci. Rep. 5 (2015), 8980. https://doi.org/10.1038/srep08980.

[2] M.G. Roberts, R.I. Hickson, J.M. McCaw, et al. A simple influenza model with complicated dynamics, J. Math. Biol. 78 (2018), 607–624. https://doi.org/10.1007/s00285-018-1285-z.

[3] C.A. Beauchemin, A. Handel, A review of mathematical models of influenza A infections within a host or cell culture: lessons learned and challenges ahead, BMC Public Health 11 (2011), S7. https://doi.org/10.1186/1471-2458-11-s1-s7.

[4] N.S. Chong, J.M. Tchuenche, R.J. Smith, A mathematical model of avian influenza with half-saturated incidence, Theory Biosci. 133 (2013), 23–38. https://doi.org/10.1007/s12064-013-0183-6.

[5] C. Quirouette, N.P. Younis, M.B. Reddy, et al. A mathematical model describing the localization and spread of influenza A virus infection within the human respiratory tract, PLoS Comput. Biol. 16 (2020), e1007705. https://doi.org/10.1371/journal.pcbi.1007705.

[6] I.A. Baba, H. Ahmad, M.D. Alsulami, et al. A mathematical model to study resistance and non-resistance strains of influenza, Results Phys. 26 (2021), 104390. https://doi.org/10.1016/j.rinp.2021.104390.

[7] B.S. Ho, K.M. Chao, On the influenza vaccination policy through mathematical modeling, Int. J. Infect. Dis. 98 (2020), 71–79. https://doi.org/10.1016/j.ijid.2020.06.043.

[8] C.W. Kanyiri, K. Mark, L. Luboobi, Mathematical analysis of influenza a dynamics in the emergence of drug resistance, Comput. Math. Methods Med. 2018 (2018), 2434560. https://doi.org/10.1155/2018/2434560.

[9] G. Hernandez-Mejia, A.Y. Alanis, E.A. Hernandez-Vargas, Inverse optimal impulsive control based treatment of influenza infection, IFAC-PapersOnLine 50 (2017), 12185–12190. https://doi.org/10.1016/j.ifacol.2017.08.2272.

[10] N. Ferguson, D. Laydon, G.N. Gilani, et al. Report 9: Impact of non-pharmaceutical interventions (NPIs) to reduce COVID19 mortality and healthcare demand, Imperial College London, 2020. https://doi.org/10.25561/77482.

[11] T. Sardar, S.S. Nadim, S. Rana, et al. Assessment of lockdown effect in some states and overall India: A predictive mathematical study on COVID-19 outbreak, Chaos Solitons Fractals. 139 (2020), 110078. https://doi.org/10.1016/j.chaos.2020.110078.

[12] J. Nainggolan, Fatmawati, Optimal prevention strategy of the type SIR COVID-19 spread model in Indonesia, Commun. Math. Biol. Neurosci., 2021 (2021), 46. https://doi.org/10.28919/cmbn/5571.

[13] J. Nainggolan, M.F. Ansori, Stability and sensitivity analysis of the COVID-19 spread with comorbid diseases, Symmetry 14 (2022), 2269. https://doi.org/10.3390/sym14112269.

[14] J. Nainggolan, J. Harianto, H. Tasman, An optimal control of prevention and treatment of COVID-19 spread in Indonesia, Commun. Math. Biol. Neurosci. 2023 (2023), 3. https://doi.org/10.28919/cmbn/7820.

[15] F. Saldaña, J.X. Velasco-Hernández, Modeling the COVID-19 pandemic: a primer and overview of mathematical epidemiology, SeMA 79 (2021), 225–251. https://doi.org/10.1007/s40324-021-00260-3.

[16] L. Pinky, H.M. Dobrovolny, Epidemiological consequences of viral interference: A mathematical modeling study of two interacting viruses, Front. Microbiol. 13 (2022), 830423. https://doi.org/10.3389/fmicb.2022.830423.

[17] S. Bhowmick, I.M. Sokolov, H.H.K. Lentz, Decoding the double trouble: A mathematical modelling of co-infection dynamics of SARS-CoV-2 and influenza-like illness, Biosystems 224 (2023), 104827. https://doi.org/10.1016/j.biosystems.2023.104827.

[18] G. González-Parra, A.J. Arenas, Mathematical modeling of SARS-CoV-2 omicron wave under vaccination effects, Computation 11 (2023), 36. https://doi.org/10.3390/computation11020036.

[19] M.M. Ojo, T.O. Benson, O.J. Peter, et al. Nonlinear optimal control strategies for a mathematical model of COVID-19 and influenza co-infection, Physica A: Stat. Mech. Appl. 607 (2022), 128173. https://doi.org/10.1016/j.physa.2022.128173.

[20] P. van den Driessche, J. Watmough, Reproduction numbers and sub-threshold endemic equilibria for compartmental models of disease transmission, Math. Biosci. 180 (2002), 29–48. https://doi.org/10.1016/s0025-5564(02)00108-6.